AGU PUBLICATIONS

Geophysical Research Letters

RESEARCH LETTER
10.1002/2015GL065262

Special Section:
First Results from the MAVEN Mission to Mars

MAVEN insights into oxygen pickup ions at Mars

A. Rahmati[1], D. E. Larson[2], T. E. Cravens[1], R. J. Lillis[2], P. A. Dunn[2], J. S. Halekas[3], J. E. Connerney[4], F. G. Eparvier[5], E. M. B. Thiemann[5], and B. M. Jakosky[5]

[1]Department of Physics and Astronomy, University of Kansas, Lawrence, Kansas, USA, [2]Space Sciences Laboratory, University of California, Berkeley, California, USA, [3]Department of Physics and Astronomy, University of Iowa, Iowa City, Iowa, USA, [4]NASA Goddard Space Flight Center, Greenbelt, Maryland, USA, [5]Laboratory for Atmospheric and Space Physics, University of Colorado Boulder, Boulder, Colorado, USA

Abstract Since Mars Atmosphere and Volatile EvolutioN (MAVEN)'s arrival at Mars on 21 September 2014, the SEP (Solar Energetic Particle) instrument on board the MAVEN spacecraft has been detecting oxygen pickup ions with energies of a few tens of keV up to ~200 keV. These ions are created in the distant upstream part of the hot atomic oxygen exosphere of Mars, via photoionization, charge exchange with solar wind protons, and electron impact. Once ionized, atomic oxygen ions are picked up by the solar wind and accelerated downstream, reaching energies high enough for SEP to detect them. We model the flux of oxygen pickup ions observed by MAVEN SEP in the undisturbed upstream solar wind and compare our results with SEP's measurements. Model-data comparisons of SEP fluxes confirm that pickup oxygen associated with the Martian exospheric hot oxygen is indeed responsible for the MAVEN SEP observations.

Key Points:
- Oxygen pickup ions are detected by MAVEN SEP in the undisturbed solar wind at Mars
- Model-data comparisons indicate pickup oxygen associated with the Martian exospheric hot oxygen
- Statistical analysis of SEP data constrains exospheric hot oxygen densities and escape at Mars

Correspondence to:
T. E. Cravens,
cravens@ku.edu

Citation:
Rahmati, A., D. E. Larson, T. E. Cravens, R. J. Lillis, P. A. Dunn, J. S. Halekas, J. E. Connerney, F. G. Eparvier, E. M. B. Thiemann, and B. M. Jakosky (2015), MAVEN insights into oxygen pickup ions at Mars, *Geophys. Res. Lett.*, *42*, doi:10.1002/2015GL065262.

Received 7 JUL 2015
Accepted 5 AUG 2015

1. Introduction

Geological and isotopic evidence suggests that in the distant past, Mars had a climate similar to the Earth, with stable liquid water on the surface, a clue to the existence of a substantial atmosphere [e.g., *Goldspiel and Squyres*, 1991; *Jakosky et al*., 1994; *Haberle*, 1998; *Malin and Edgett*, 2003]. Today, Mars has lost most of its atmosphere and is therefore unable to support water in liquid form on the surface [*Jakosky and Phillips*, 2001]. The processes involved in atmospheric escape from Mars have been extensively investigated in the past few decades [e.g., *Lundin et al*., 1989; *Brain and Jakosky*, 1998; *Chassefière and Leblanc*, 2004]. The MAVEN (Mars Atmosphere and Volatile EvolutioN) mission to Mars aims to take these studies one step further by determining the current state of the upper atmosphere, measuring the drivers of escape and quantifying the escape rates of different species [*Jakosky et al*., 2015; *Bougher et al*., 2014].

One of the major sources of neutral escape on Mars is the exothermic dissociative recombination of O_2^+ in the ionosphere, which creates two oxygen atoms, some of which obtain energies above the escape energy of ~2 eV [*Nagy and Cravens*, 1988; *Kim et al*., 1998; *Ip*, 1988]. These hot oxygen atoms may collide with neutral particles and lose energy; nonetheless, some escape the planet and comprise the extended Martian hot oxygen corona [*Feldman et al*., 2011; *Fox and Hać*, 2014; *Rahmati et al*., 2014].

The hot oxygen exosphere of Mars resembles a comet's coma in that both are very extensive [*Cravens et al*., 2002; *Nagy et al*., 2004]. A heavy ion (e.g., oxygen, water group) created in the far upstream part of these extended media and picked up by the solar wind will have enough space to reach the peak of its gyromotion and obtain the maximum pickup energy [*Coates*, 2004; *Goldstein et al*., 2015]. Depending on solar wind conditions, this energy can be in excess of tens of keV, thus detectable by solid state detectors. The Tunde-M solid state detector on the Vega 1 spacecraft detected water group pickup ions outside the bow shock of comet Halley [*Kecskemety et al*., 1989]. The SLED (solar low-energy detector) solid state detector on board the Phobos 2 spacecraft also detected oxygen pickup ions in the vicinity of Mars [*Cravens et al*., 2002]. It was predicted by *Rahmati et al*. [2014] that the SEP (Solar Energetic Particle) (D. E. Larson et al., The MAVEN solar energetic particle investigation, submitted to *Space Science Reviews*, 2015) instrument on MAVEN would also be able to detect oxygen pickup ions at Mars.

MAVEN SEP was turned on during the cruise phase and observed energetic particles of solar origin, associated with interplanetary shocks due to coronal mass ejections and solar flares. Soon after the spacecraft was inserted into Martian orbit on 21 September 2014, SEP started to detect additional significant counts in its lower energy channels, i.e., ~10–100 keV that were qualitatively different from the SEPs detected in interplanetary space in

energy spectrum and temporal behavior. The count rates correlated with solar wind speed, as well as with the angle between the solar wind bulk flow velocity and the IMF (interplanetary magnetic field) direction. This paper describes this correlation, along with further model-data comparisons that include SEP's instrumental geometry and energy response. This strongly implies that these counts are signatures of energetic oxygen pickup ions of Martian exospheric origin.

2. Pickup Oxygen Model

Test particle simulations have been utilized in the past in order to calculate fluxes of pickup ions in different space environments [e.g., *Cravens*, 1989; *Luhmann and Kozyra*, 1991; *Kallio and Koskinen*, 1999; *Fang et al*., 2008; *Curry et al*., 2014; *Gronoff et al*., 2014]. Test particle simulations of oxygen pickup ions at Mars create many oxygen ions with probabilities proportional to the ionization rate of neutral oxygen at random locations around Mars. The number of particles simulated in different studies ranges between thousands to billions, depending on resolution requirements and computational resources. After creating each particle, the codes then numerically solve the equations of motion of the particles, calculating their trajectory in the background electric and magnetic fields. The fields are usually adopted from MHD or hybrid simulations and assumed to be static, i.e., not updated in each time step of the simulation. Certain planar bins are placed in specific locations to record the velocity components of particles crossing the bins. The number of particles crossing each bin along with their associated velocities are used to calculate the flux of particles in each bin.

In certain cases when MAVEN is in the upstream undisturbed solar wind, one can use the uniform IMF components measured by the MAVEN MAG (magnetometer) instrument [*Connerney et al*., 2015] and analytically solve the equations of motion of the pickup ions in upstream fields. This eliminates the need for the computationally intensive task of numerically solving the equations of motion and results in much faster run times. This approach enabled us to extend the creation point of our pickup ions to very high altitudes, as far as 300,000 km, to ensure that the full gyromotion of the pickup ions is captured in our simulations. We were also able to run multiple simulations for consecutive 30 s time intervals, during the periods when MAVEN was in the upstream solar wind. The 30 s averaged drivers, i.e., solar wind velocities, densities, and IMF components, were fed into each simulation run for which pickup oxygen fluxes were computed. Utilizing drivers with a time resolution higher than 30 s would not, however, provide higher fidelity results, because pickup ions experience a varying field over their gyromotion and in effect "average" the fields over their gyroperiod before they reach MAVEN. It is worth mentioning that typical gyroradii and gyroperiods for pickup oxygen in the undisturbed solar wind are on the order of 10,000–50,000 km and 30–150 s, respectively.

The dayside exospheric neutral oxygen used in our simulations is a time-independent hemispherically symmetric exosphere, calculated using the combination of a two-stream simulation of hot oxygen transport and the Liouville theorem for the Martian dayside [*Rahmati et al*., 2014]. The sources of ionization in the hot oxygen exosphere of Mars are photoionization of neutral oxygen atoms by the solar extreme ultraviolet radiation and charge exchange of neutral oxygen atoms with solar wind protons. Electron impact ionization plays a minor role in ionizing neutral oxygen in solar wind [*Cravens et al*., 1987]. Ionization rates due to photoionization and charge exchange are calculated using equations (1) and (2), respectively.

$$I_{\mathrm{PI}} = n_{\mathrm{O}} \int \sigma_{\mathrm{PI}}(\lambda)\ \ \phi_{\mathrm{EUV}}(\lambda)\ \ \mathrm{d}\lambda \tag{1}$$

$$I_{\mathrm{CX}} = n_{\mathrm{O}}\ \sigma_{\mathrm{CX}} n_{\mathrm{H+}} U_{\mathrm{sw}} \tag{2}$$

where n_{O} is the neutral atomic oxygen density, adopted from *Rahmati et al*. [2014], $\sigma_{\mathrm{PI}}(\lambda)$ is the wavelength-dependent photoionization cross section for atomic oxygen, adopted from *Angel and Samson* [1988], $\phi_{\mathrm{EUV}}(\lambda)$ is the solar EUV (extreme ultraviolet) spectrum, calculated by the FISM (Flare Irradiance Spectral Model) [*Chamberlin et al*., 2007], which uses MAVEN EUV monitor [*Eparvier et al*., 2015] measurements as proxy, λ is the solar photon wavelength, σ_{CX} is the cross section for charge exchange between a solar wind proton and an oxygen atom, adopted from *Stebbings et al*. [1964], and $n_{\mathrm{H+}}$ and U_{sw} are the solar wind proton density and velocity, respectively, both measured by MAVEN SWIA (Solar Wind Ion Analyzer) [*Halekas et al*., 2013]. Given that the solar wind He^{++}/H^{+} ratio is typically below 10%, the charge exchange between He^{++} and oxygen atoms was neglected in our model.

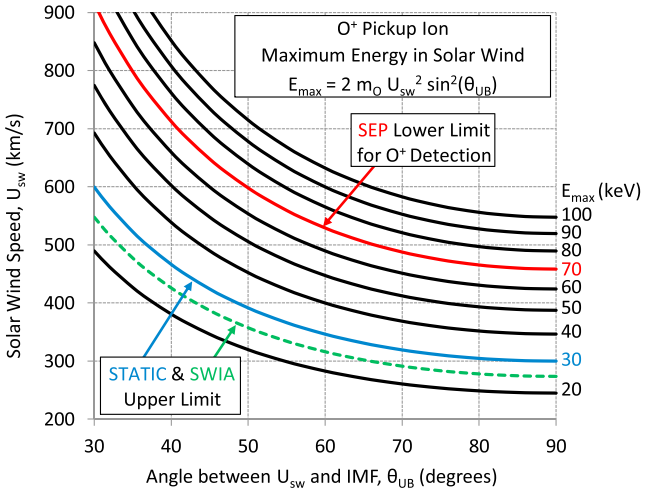

Figure 1. Contours of maximum pickup oxygen energy versus solar wind speed and the angle between the solar wind velocity and the IMF direction.

Once ionized, each oxygen ion is acted upon by the solar wind embedded magnetic field and the corresponding motional electric field. The ions are "picked up" by these fields and form a ring-beam distribution in velocity space due to gyration about the magnetic field lines. The maximum energy that a pickup ion can achieve is given by the expression

$$E_{max} = 2\ m_O U_{sw}^2 \sin^2(\theta_{UB}) \qquad (3)$$

where m_O is the mass of atomic oxygen and θ_{UB} is the angle between the solar wind velocity and the IMF direction. In certain conditions when θ_{UB} is close to 90°, pickup ions can be accelerated to a maximum velocity of twice that of the solar wind. Figure 1 shows contours of pickup oxygen maximum energy as a function of U_{sw} and θ_{UB}. MAVEN SEP, as described in the following section, is able to detect oxygen ions with energies above ~70 keV, and thus, solar wind velocities above ~500 km/s with large angles between the solar wind and the IMF direction are needed.

Our pickup ion code places a bin at the position of MAVEN at 30 s time intervals and calculates the flux of incoming pickup ions crossing that bin. Figure 2 shows three examples of the model pickup ion spectrum for three different solar wind conditions at an altitude of 6000 km upstream of the Martian subsolar point, with an assumed IMF strength of 5 nT and a total ionization frequency of $4.5 \times 10^{-7}\ s^{-1}$. The figure illustrates how pickup oxygen fluxes vary as a function of U_{sw} and θ_{UB}. These fluxes have to be convolved with SEP's energy response, field of view (FOV), and detector effective area. Therefore, SEP will only be able to detect part of the pickup oxygen flux due to its limited energy response and FOV.

3. MAVEN SEP

MAVEN SEP is a solid state telescopic detector designed to measure the flux of solar energetic particles during solar particle events, e.g., during the passage of an interplanetary coronal mass ejection. High-energy particle observations made by SEP can be used to determine the effects of energy deposition in the Martian upper atmosphere and to quantify the role of solar particle events in atmospheric escape from Mars. SEP can also be used as an energetic oxygen pickup ion detector.

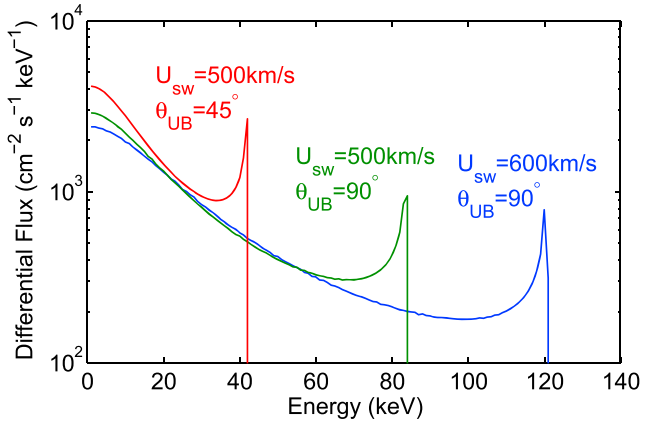

Figure 2. Model pickup oxygen fluxes for three different solar wind and IMF conditions. The parameter U_{sw} is the solar wind speed and θ_{UB} is the angle between the solar wind and the magnetic field. The rest of the simulation parameters described in the text are held constant for all three cases.

There are two SEP sensors mounted on MAVEN, each containing two double-ended telescopes with perpendicular look directions. Each of the four telescopes consists of a stack of three silicon detectors that detect primarily ions at one end (called "open," where a strong magnet sweeps away electrons below ~250 keV) and electrons in the other end (called "foil," where a thin foil stops ions below ~250 keV). A third silicon layer (called "thick") in the middle of the open and the foil detectors is used to detect the highest-energy ions/electrons that penetrate the open/foil detector. Oxygen

pickup ions are detected in the open detectors that have a look direction in the sunward hemisphere; therefore, in the rest of this paper we only describe the two open "front" detectors (namely, SEP1F and SEP2F), and will show the corresponding data.

Oxygen ions that enter SEP lose part of their energy in the aluminum coating and the silicon dead layers at the front edge of the open detectors, as well as due to the pronounced effects of pulse height defect for heavy ions. These effects were simulated using the Geant4 software package [*Agostinelli et al*., 2003; *Allison et al*., 2006], and the energy response of each detector to oxygen ions was calculated individually. Oxygen ions entering SEP1F and SEP2F deposit energies that are on average ~50 keV lower than their incident energy; and since SEP's electronic noise threshold is 11 keV, oxygen ions with energies above ~60 keV trigger counts. It is also worth noting that SEP detects protons with energies above ~20 keV and is therefore blind to the solar wind protons, as well as pickup protons of Martian hydrogen exosphere origin in the undisturbed solar wind.

The FOV of SEP is a rectangle spanning 31° at the center and 42° at the corners of the rectangular FOV. For simplicity, in our model we assumed the FOV to be a cone with an opening angle of 40°. SEP's effective detection area is ~1 cm^2 at the center of the FOV, with a reduction in the area at the edges of the FOV, and we included this effect in the model. Furthermore, oxygen ions entering SEP near the edge of the FOV cross a slightly thicker dead layer, therefore losing more energy compared to those entering through the middle of the FOV. We found this to be a negligible effect and ignored it in our simulations.

SEP open detectors have a total of 30 energy bins, 12 of which span the 10–100 keV range, which is where pickup oxygen is detected. The energy resolution of SEP is $\Delta E/E \sim 30\%$. We assumed that there is no bleeding and/or double counting between the neighboring energy bins and binned our simulated fluxes similar to SEP's energy bins. Pickup oxygen fluxes were convolved with SEP's energy response and its FOV-dependent effective detection area to obtain count rates. SEP's attenuators reduce the detection area by about 2 orders of magnitude; therefore, we multiplied the measured count rates by a factor of 100 when SEP's attenuators were closed, an approximation which is adequate for our qualitative comparison. Further Geant4 simulations for SEP with closed attenuators will lead to a more quantitative analysis of pickup oxygen fluxes.

4. Model-Data Comparison

During a few days in December of 2014, the solar wind reached speeds higher than 500 km/s and the SEP instrument was able to detect energetic oxygen pickup ions. For these days, we analyzed parts of the orbits when MAVEN was in the undisturbed upstream solar wind to compare our model results with the data. Oxygen pickup ions were absent in both the data and model results during times of slower solar wind. Figure 3 shows a 1 h time period starting at 14:30 UTC on 2 December 2014, when the solar wind speed was ~525 km/s. Figure 3a shows the three components of the IMF measured by MAVEN MAG in MSO (Mars-Solar-Orbital) coordinates, Figure 3b shows the calculated angle between the solar wind velocity and the magnetic field, and Figure 3c shows the maximum energy that oxygen pickup ions can achieve (E_{max}), calculated using equation (3).

The SEP-measured and SEP-modeled pickup oxygen spectrograms for SEP2F are presented in Figures 3d and 3e, respectively. A good agreement is found between our model results and the data, confirming detection of pickup oxygen associated with the Martian extended hot oxygen exosphere. In particular, the fluctuations in the maximum energy calculated in Figure 3c can be observed in both the data and model results. For the whole time period shown in Figure 3, SEP2F had the Sun in its FOV, and its attenuators were closed. The dips in E_{max} are well correlated with the departures of θ_{UB} from 90°, which is represented by the dashed line in Figure 3b. The energy dips also appear in both SEP-measured and SEP-modeled pickup oxygen fluxes, the most obvious of which is seen at the 27 min mark. Note that our model predicts features to appear slightly ahead of time, i.e., on the order of a half gyroperiod compared to the data. This is because accelerating pickup ions lag behind the solar wind during the time it takes them to reach E_{max}.

As seen in Figure 3a, the IMF has a Y component of about -5 nT, with X and Z components fluctuating around zero. Therefore, according to $\mathbf{E} = -\mathbf{U}_{sw} \times \mathbf{B}$, the motional electric field experienced by newly born pickup ions is in the $-Z$ direction and oxygen ions begin their trajectory parallel to this field. As pickup ions gyrate about $\mathbf{B}$ and gain energy, their $-X$ (Sun-Mars direction) velocity component increases and they begin to enter SEP2F's FOV near the peak of their gyromotion. Therefore, for this time period, SEP2F only detects pickup ions of highest energy, thus, a "band" of energy is seen in SEP2F's spectrogram.

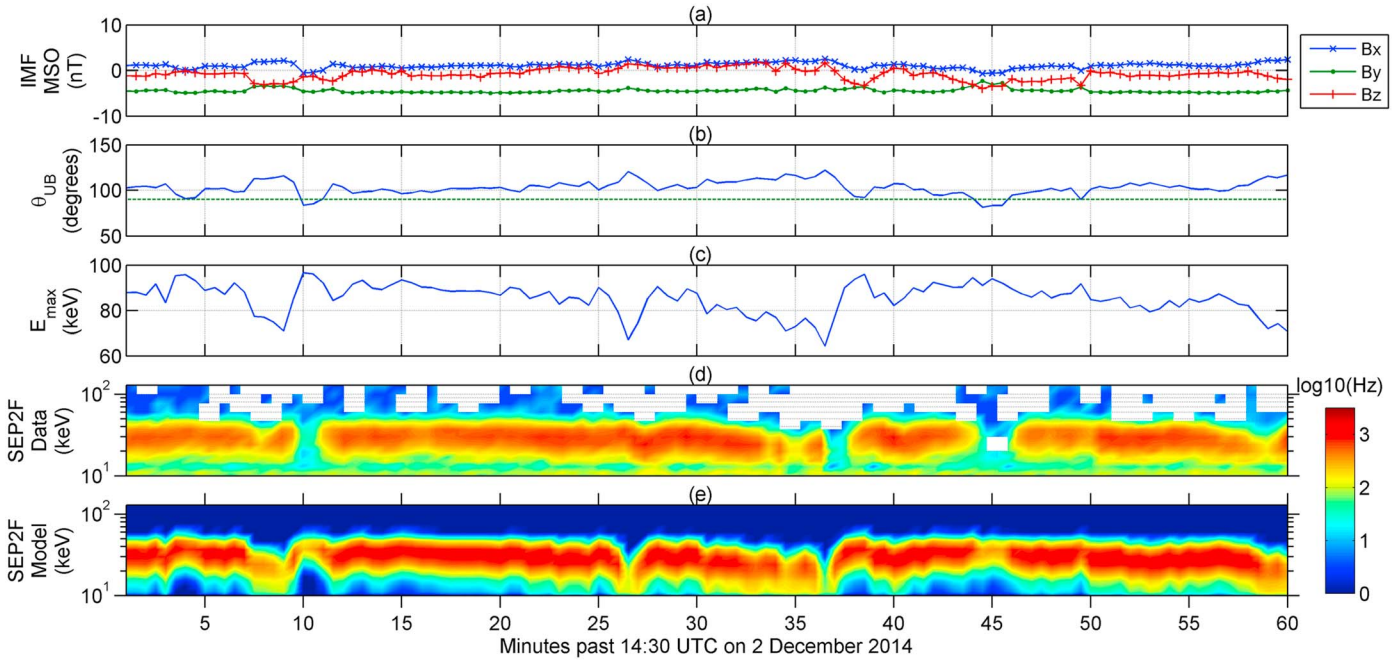

Figure 3. Model-data comparison of SEP-detected oxygen pickup ions. (a) The three components of the magnetic field measured by MAVEN MAG; (b) the calculated angle between the solar wind velocity and the magnetic field, with the dashed line representing an IMF perpendicular to the solar wind; (c) the maximum energy that oxygen pickup ions can achieve (E_{max}); pickup oxygen count rate spectrograms for SEP1F (d) measured and (e) model results.

Figure 4 shows the measured and modeled SEP2F count rates for the 30 min mark of Figure 3 (2 December 2014, 15:00 UTC). At this time step, the incident E_{max} for oxygen pickup ions is 90 keV, and the deposited energy associated with this E_{max} and calculated using SEP's energy response is 40 ± 10 keV. The best agreement between the data and the model is also found for the same range of energies. Lower energy pickup ions in the ring-beam distribution approach the edges of the FOV, causing an increase in the uncertainties associated with detector edge effects (e.g., ion scattering, increased dead-layer thickness, and reduced detector effective area). Also, the higher count rates in the low energy part of the data are noise from solar photons entering SEP2F, which had a near sunward look direction during the selected time period. Note that SEP1F had a look direction perpendicular to the Mars-Sun line, and neither the measurements nor our model show signatures of pickup oxygen detection in SEP1F.

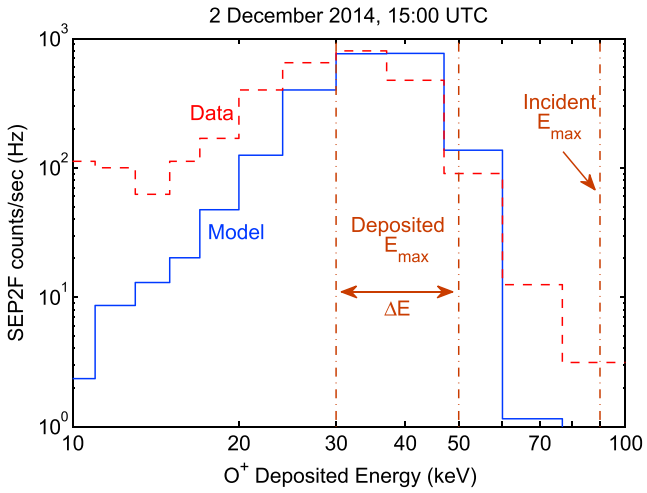

Figure 4. SEP2F measured (red) and modeled (blue) count rates for 2 December 2014, 15:00 UTC. The incident maximum energy (E_{max}) and the corresponding deposited energy full width at half maximum (FWHM = ΔE) associated with E_{max} are also shown.

On 28 December 2014, the solar wind speed reached 600 km/s and both SEP1F and SEP2F detected pickup oxygen. Figure 5 shows a 90 min time period starting at 00:10 UTC during which SEP1F and SEP2F had look angles that were 45° to the west and east of the Mars-Sun line, respectively. Figures 5a to 5c are as described in Figure 3, Figures 5d and 5e are the measured count rates by SEP1F and SEP2F, respectively, and Figures 5f and 5g are model results for SEP1F and SEP2F, respectively. The IMF direction determines the trajectories of pickup ions, and our model correctly predicts which SEP has the pickup ring-beam distribution in its FOV. The time periods during

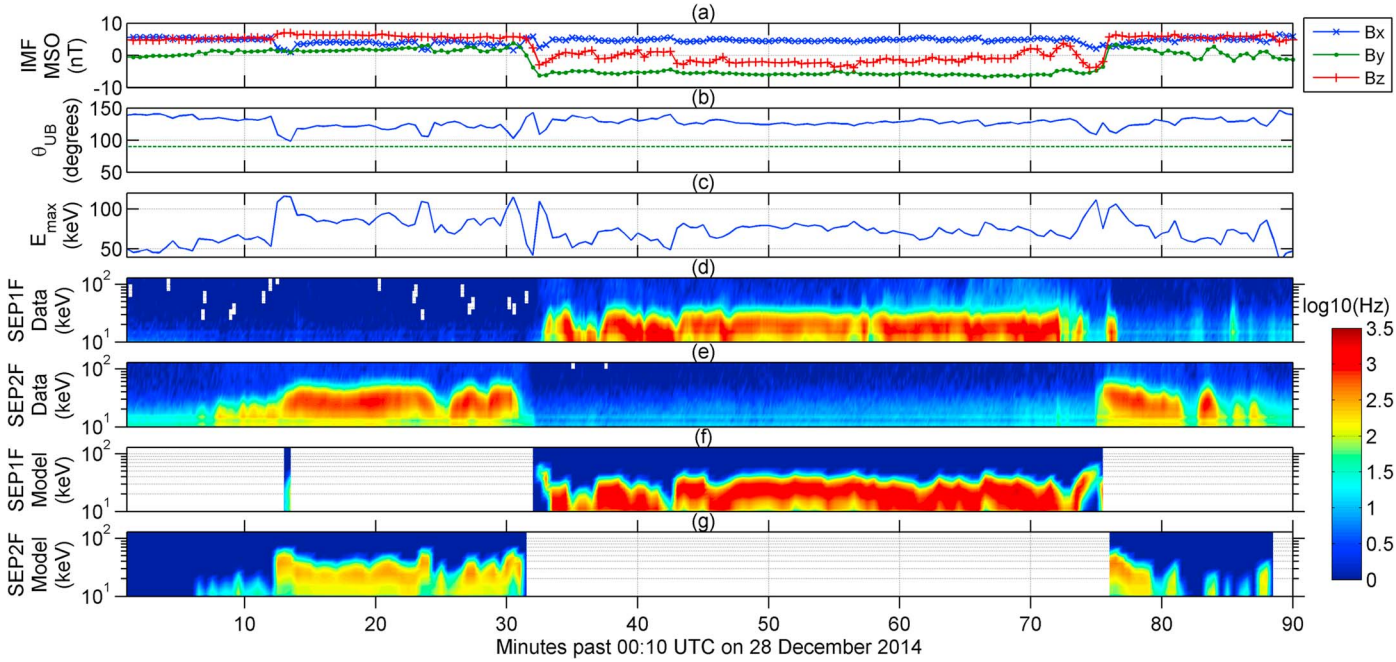

Figure 5. Model-data comparison of SEP-detected oxygen pickup ions. (a) The three components of the magnetic field measured by MAVEN MAG; (b) the calculated angle between the solar wind velocity and the magnetic field, with the dashed line representing an IMF perpendicular to the solar wind; (c) the maximum energy that oxygen pickup ions can achieve (E_{max}); pickup oxygen count rate spectrograms for (d) SEP1F and (e) SEP2F measured as well as (f) SEP1F and (g) SEP2F model results.

which the pickup ring-beam distribution was outside the FOV of each SEP are depicted as white space in the model spectrograms.

5. Discussion

The agreement between our oxygen pickup ion model and the SEP data confirms detection of pickup oxygen associated with the distant hot oxygen exosphere of Mars. Pickup oxygen ions detected by SEP begin their trajectory 10 to 100 Martian radii upstream of Mars, depending on which part of the pickup ring-beam distribution is in the FOV of SEP, as well as on the pickup gyroradius, which is dictated by the solar wind speed, and the IMF strength and direction. Since pickup oxygen fluxes are directly proportional to atomic oxygen densities at the locations where pickup ions are born, statistical analysis of SEP measurements over the course of the entire MAVEN mission will enable the exospheric neutral oxygen densities to be constrained at different locations upstream of Mars.

MAVEN SWIA and STATIC (Suprathermal and Thermal Ion Composition) have maximum ion detection energy limits of 25 keV and 30 keV, respectively, and therefore are blind to the higher-energy part of the pickup oxygen distribution, which is associated with ions created in the distant and mainly escaping part of the Martian exosphere [*Rahmati et al.*, 2014]. These instruments are, on the other hand, able to measure the 3-D distribution of the lower energy pickup ions, which are created closer to Mars. In addition, STATIC (J. P. McFadden et al., The MAVEN Suprathermal and Thermal Ion Composition (STATIC) instrument, submitted to *Space Science Reviews*, 2015) includes mass discrimination capability and can be used to distinguish between pickup ions of different species. However, the lower geometric factor of SWIA and STATIC compared to SEP, which has a geometric factor of 0.18 cm^2 sr, renders them less suitable for obtaining signatures of pickup oxygen when MAVEN is near its dayside apoapsis (~3000–6000 km), due to lower pickup ion fluxes at those high altitudes.

Due to the narrow FOV of SEP, only a small part of the neutral exosphere of Mars is being probed by SEP at each time. For the time step shown in Figure 4 (2 December 2014, 15:00 UTC), oxygen pickup ions entering SEP's FOV originate from MSO coordinates of $[x, y, z] = [60, 17, 34] \times 10^3$ km, or a radial distance of 70×10^3 km (20 Martian radii). The exospheric neutral density associated with this distance, according to *Rahmati et al.* [2014], is ~2 cm^{-3}; however, their model assumed spherical symmetry and used ionospheric inputs from pre-MAVEN data sets. Utilizing MAVEN-measured parameters in exospheric models will provide a new set

of photochemical oxygen escape rates. Since the distant part of the Martian exosphere is mainly escaping [*Rahmati et al.*, 2014], model-data comparisons with SEP-measured pickup oxygen fluxes provide better constraints on exospheric models and their associated neutral oxygen escape rates.

Acknowledgments
All data shown in the figures can be obtained from the corresponding author. MAVEN data are in the Planetary Data System. This work was supported by NASA grant NNH10CC04C to the University of Colorado and by subcontract to the University of Kansas. The MAVEN project is supported by NASA through the Mars Exploration Program.

The Editor thanks two anonymous reviewers for their assistance in evaluating this paper.

References

Agostinelli, S., et al. (2003), GEANT4—A simulation toolkit, *Nucl. Instrum. Methods*, *506*(3), 250–303, doi:10.1016/S0168-9002(03)01368-8.
Allison, J., et al. (2006), Geant4 developments and applications, *IEEE Trans. Nucl. Sci.*, *53*(1), 270–278, doi:10.1109/TNS.2006.869826.
Angel, G. C., and J. A. Samson (1988), Total photoionization cross sections of atomic oxygen from threshold to 44.3 Å, *Phys. Rev. A*, *38*(11), 5578, doi:10.1103/PhysRevA.38.5578.
Bougher, S. W., T. E. Cravens, J. Grebowsky, and J. Luhmann (2014), The aeronomy of Mars: Characterization by MAVEN of the upper atmosphere reservoir that regulates volatile escape, *Space Sci. Rev.*, doi:10.1007/s11214-014-0053-7.
Brain, D. A., and B. M. Jakosky (1998), Atmospheric loss since the onset of the Martian geologic record: Combined role of impact erosion and sputtering, *J. Geophys. Res.*, *103*(E10), 22,689–22,694, doi:10.1029/98JE02074.
Chamberlin, P. C., T. N. Woods, and F. G. Eparvier (2007), Flare Irradiance Spectral Model (FISM): Daily component algorithms and results, *Space Weather*, *5*, S07005, doi:10.1029/2007SW000316.
Chassefière, E., and F. Leblanc (2004), Mars atmospheric escape and evolution; interaction with the solar wind, *Planet. Space Sci.*, *52*(11), 1039–1058, doi:10.1016/j.pss.2004.07.002.
Coates, A. J. (2004), Ion pickup at comets, *Adv. Space Res.*, *33*(11), 1977–1988, doi:10.1016/j.asr.2003.06.029.
Connerney, J. E. P., J. Espley, P. Lawton, S. Murphy, J. Odom, R. Oliversen, and D. Sheppard (2015), The MAVEN magnetic field investigation, *Space Sci. Rev.*, doi:10.1007/s11214-015-0169-4.
Cravens, T. E. (1989), Test particle calculations of pick-up ions in the vicinity of comet Giacobini-Zinner, *Planet. Space Sci.*, *37*(10), 1169–1184, doi:10.1016/0032-0633(89)90012-3.
Cravens, T. E., J. U. Kozyra, A. F. Nagy, T. I. Gombosi, and M. Kurtz (1987), Electron impact ionization in the vicinity of comets, *J. Geophys. Res.*, *92*(A7), 7341–7353, doi:10.1029/JA092iA07p07341.
Cravens, T. E., A. Hoppe, S. A. Ledvina, and S. McKenna-Lawlor (2002), Pickup ions near Mars associated with escaping oxygen atoms, *J. Geophys. Res.*, *107*(A8), 1170, doi:10.1029/2001JA000125.
Curry, S. M., M. Liemohn, X. Fang, Y. Ma, J. Slavin, J. Espley, S. Bougher, and C. F. Dong (2014), Test particle comparison of heavy atomic and molecular ion distributions at Mars, *J. Geophys. Res. Space Physics*, *119*, 2328–2344, doi:10.1002/2013JA019221.
Eparvier, F. G., P. C. Chamberlin, T. N. Woods, and E. M. B. Thiemann (2015), The solar extreme ultraviolet monitor for MAVEN, *Space Sci. Rev.*, doi:10.1007/s11214-015-0195-2.
Fang, X., M. W. Liemohn, A. F. Nagy, Y. Ma, D. L. De Zeeuw, J. U. Kozyra, and T. H. Zurbuchen (2008), Pickup oxygen ion velocity space and spatial distribution around Mars, *J. Geophys. Res.*, *113*, A02210, doi:10.1029/2007JA012736.
Feldman, P. D., et al. (2011), Rosetta-Alice observations of exospheric hydrogen and oxygen on Mars, *Icarus*, *214*(2), 394–399, doi:10.1016/j.icarus.2011.06.013.
Fox, J. L., and A. B. Hać (2014), The escape of O from Mars: Sensitivity to the elastic cross sections, *Icarus*, *228*, 375–385, doi:10.1016/j.icarus.2013.10.014.
Goldspiel, J. M., and S. W. Squyres (1991), Ancient aqueous sedimentation on Mars, *Icarus*, *89*(2), 392–410, doi:10.1016/0019-1035(91)90186-W.
Goldstein, R., et al. (2015), The Rosetta Ion and Electron Sensor (IES) measurement of the development of pickup ions from comet 67P/Churyumov-Gerasimenko, *Geophys. Res. Lett.*, *42*, 3093–3099, doi:10.1002/2015GL063939.
Gronoff, G., A. Rahmati, C. S. Wedlund, C. J. Mertens, T. E. Cravens, and E. Kallio (2014), The precipitation of keV energetic oxygen ions at Mars and their effects during the comet Siding Spring approach, *Geophys. Res. Lett.*, *41*, 4844–4850, doi:10.1002/2014GL060902.
Haberle, R. M. (1998), Early Mars climate models, *J. Geophys. Res.*, *103*(E12), 28,467–28,479, doi:10.1029/98JE01396.
Halekas, J. S., E. R. Taylor, G. Dalton, G. Johnson, D. W. Curtis, J. P. McFadden, D. L. Mitchell, R. P. Lin, and B. M. Jakosky (2013), The solar wind ion analyzer for MAVEN, *Space Sci. Rev.*, doi:10.1007/s11214-013-0029-z.
Ip, W. H. (1988), On a hot oxygen corona of Mars, *Icarus*, *76*(1), 135–145, doi:10.1016/0019-1035(88)90146-7.
Jakosky, B. M., and R. J. Phillips (2001), Mars' volatile and climate history, *Nature*, *412*(6843), 237–244, doi:10.1038/35084184.
Jakosky, B. M., R. O. Pepin, R. E. Johnson, and J. L. Fox (1994), Mars atmospheric loss and isotopic fractionation by solar-wind-induced sputtering and photochemical escape, *Icarus*, *111*(2), 271–288, doi:10.1006/icar.1994.1145.
Jakosky, B. M., et al. (2015), The Mars Atmosphere and Volatile Evolution (MAVEN) mission, *Space Sci. Rev.*, doi:10.1007/s11214-015-0139-x.
Kallio, E., and H. Koskinen (1999), A test particle simulation of the motion of oxygen ions and solar wind protons near Mars, *J. Geophys. Res.*, *104*(A1), 557–579, doi:10.1029/1998JA900043.
Kecskemety, K., et al. (1989), Pickup ions in the unshocked solar wind at comet Halley, *J. Geophys. Res.*, *94*(A1), 185–196, doi:10.1029/JA094iA01p00185.
Kim, J., A. F. Nagy, J. L. Fox, and T. E. Cravens (1998), Solar cycle variability of hot oxygen atoms at Mars, *J. Geophys. Res.*, *103*(A12), 29,339–29,342, doi:10.1029/98JA02727.
Luhmann, J. G., and J. U. Kozyra (1991), Dayside pickup oxygen ion precipitation at Venus and Mars: Spatial distributions, energy deposition and consequences, *J. Geophys. Res.*, *96*(A4), 5457–5467, doi:10.1029/90JA01753.
Lundin, R., A. Zakharov, R. Pellinen, H. Borg, B. Hultqvist, N. Pissarenko, E. M. Dubinin, S. W. Barabash, I. Liede, and H. Koskinen (1989), First measurements of the ionospheric plasma escape from Mars, *Nature*, *341*(6243), 609–612, doi:10.1038/341609a0.
Malin, M. C., and K. S. Edgett (2003), Evidence for persistent flow and aqueous sedimentation on early Mars, *Science*, *302*(5652), 1931–1934, doi:10.1126/science.1090544.
Nagy, A. F., and T. E. Cravens (1988), Hot oxygen atoms in the upper atmospheres of Venus and Mars, *Geophys. Res. Lett.*, *15*(5), 433–435, doi:10.1029/GL015i005p00433.
Nagy, A. F., et al. (2004), The plasma environment of Mars, *Space Sci. Rev.*, *111*, 33–114, doi:10.1023/B:SPAC.0000032718.47512.92.
Rahmati, A., T. E. Cravens, A. F. Nagy, J. L. Fox, S. W. Bougher, R. J. Lillis, S. A. Ledvina, D. E. Larson, P. Dunn, and J. A. Croxell (2014), Pickup ion measurements by MAVEN: A diagnostic of photochemical oxygen escape from Mars, *Geophys. Res. Lett.*, *41*, 4812–4818, doi:10.1002/2014GL060289.
Stebbings, R. F., A. C. H. Smith, and H. Ehrhardt (1964), Charge transfer between oxygen atoms and O+ and H+ ions, *J. Geophys. Res.*, *69*(11), 2349–2355, doi:10.1029/JZ069i011p02349.